

GFP SENSORS

Peter M. Haggie^{*†} and A.S. Verkman^{*}

2.1. INTRODUCTION

The green fluorescent protein (GFP) and related genetically-encoded fluorescent proteins have had a major impact in cell biology. GFP has diverse applications in studies of protein localization, dynamics, interactions and regulation. GFP is targetable to specific cellular sites in cell culture models and *in vivo* in a wide variety of organisms. A unique application of fluorescent proteins is their engineering as real-time cellular sensors of pH, ion concentrations, second messengers, enzyme activities and other parameters. Compared to classical chemical probes, genetically-encoded fluorescent proteins permit stable non-invasive staining of specific subcellular sites in cell culture models and *in vivo* with little or no cellular toxicity. This chapter reviews the paradigms that have been developed for engineering of GFP-based sensors, applications of available sensors, and directions for further sensor development.

2.2. GENERAL PRINCIPLES OF ENGINEERING FLUORESCENT PROTEIN SENSORS

Figure 2.1 depicts several strategies that have been applied to the design of genetically-encoded fluorescent sensors. The simplest sensors (Class I) are fluorescent proteins that without modification (other than mutagenesis of primary sequence) sense a physiological parameter. Examples of intrinsic fluorescent sensors include GFP sensors of pH and chloride concentration. The steady-state fluorescence of the original (wildtype) GFP and most common GFP mutants is pH-dependent because of protonation-deprotonation of the GFP chromophore (1-4). Many yellow fluorescent proteins (YFPs) are intrinsically sensitive to halides by a mechanism involving halide-dependent shifts in pK_a (5, 6).

^{*} Departments of Medicine and Physiology, Cardiovascular Research Institute, University of California, San Francisco, CA, 94143-0521.

[†] Correspondence to: Alan S. Verkman, M.D., Ph.D. 1246 Health Sciences East Tower, Cardiovascular Research Institute, University of California, San Francisco, CA 94143-0521, U.S.A., Phone: (415)-476-8530; Fax: (415)-665-3847, E-mail: verkman@itsa.ucsf.edu; Internet: <http://www.ucsf.edu/verklab>

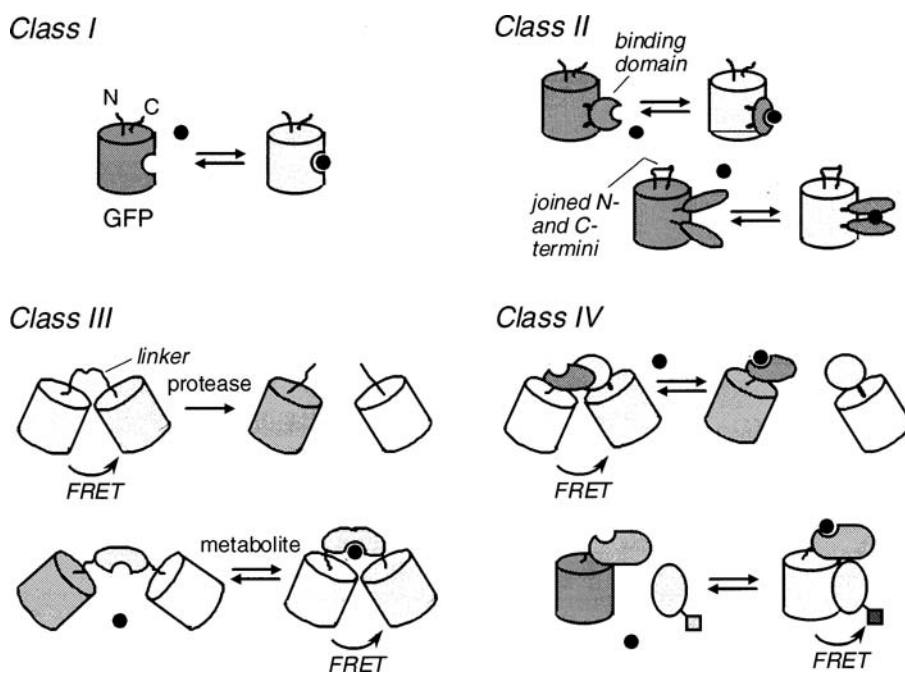


Figure 2.1. Classes of fluorescent protein-based sensors. Class I sensors consist of GFP (or other fluorescent proteins) that intrinsically respond to a parameter of interest (shown as ●). Halide and pH probes belong to this class. Class II sensors contain an additional domain or domains grafted onto GFP. Two examples of class II calcium sensors are shown: Camgaroo (*top*) contains a CaM domain (gray) inserted at residue Y145 of YFP; Pericam and G-CaMP sensors (*bottom*) contain CaM and M13 fragments joined to the new termini of circularly permuted GFP (see text for explanations). Class III sensors use intramolecular fluorescence resonance energy transfer (FRET). Donor/acceptor pairs are joined by an engineered linker that undergoes a conformational change to alter the separation/orientation of the GFP pair. Examples of class III sensors include protease sensors (*top*) that irreversibly lose FRET upon protease-mediated cleavage, and metabolite sensors (*bottom*) that undergo conformational changes upon substrate binding. Class IV sensors are FRET-based using intermolecular interactions. A cAMP sensor has been described that is composed of regulatory and catalytic subunits of PKA separately joined to donor/acceptor pairs that dissociate upon cAMP binding (*top*). A PKC sensor contained a PKC-GFP fusion protein that upon activation and threonine phosphorylation binds to a specific Cy3-tagged antibody.

Class II sensors consist of fluorescent proteins linked to an additional protein domain or domains. Here the grafted domain(s) sense changes in analyte concentration or some other parameter, producing altered protein fluorescence by conformational changes or other interactions. The newer calcium sensors such as camgaroo, G-CaMP and pericam (7-9) and voltage sensors (10, 11) belong to this class. The grafted domains can reside within or outside of the GFP primary sequence. The development of sensors containing embedded peptide sequences has exploited circular permutation as a strategy to identify regions in GFP that are tractable to protein domain insertion. Proteins containing nearby

amino- and carboxy-termini are amenable to circular permutation, where overall primary sequence connectivity of a protein is maintained whilst altering the protein termini (12). cDNA coding sequences are circularized, treated with low concentrations of DNAase to create randomly-permuted linear DNA fragments, and subcloned for expression and screening. Circular permutation of GFPs and the development of new fluorescent variants was reported in 1999 by two groups (7, 13). Using this approach with GFP, Baird *et al.* (7) determined that any of ten residues could serve as new starting amino acids, and that exogenous peptides could be inserted at specific sites without loss of fluorescence. In some cases permutation of fluorescent proteins has increased the magnitude of response of a sensor substantially, probably because the permuted fluorescent protein with new termini is better able to transduce conformational changes in grafted domains to the chromophore.

Class III sensors form the largest and most diverse family of probes and exploit changes in intramolecular fluorescence resonance energy transfer (FRET) efficiency between spectrally distinct fluorescent proteins. Intramolecular FRET sensors use an engineered linker that undergoes a conformational change to separate and/or reorient the GFP moieties, having the advantage that stoichiometries of fluorophores are strictly maintained. A simple example of a class III FRET-based sensor is a donor/acceptor GFP pair linked by a protease-cleavable sequence (14-16). Protease cleavage of the sensor irreversibly abolishes FRET as the donor and acceptor GFPs separate. Class III sensors have been described for calcium (17, 18), metabolites (19, 20) and kinase activities (21, 22), each utilizing domains for analyte binding or phosphorylation inserted between GFP donor/acceptor pairs. Upon analyte binding or phosphorylation, separation and/or orientation of the GFP donor/acceptor pair is altered with consequent changes in FRET efficiency.

Class IV sensors rely on intermolecular FRET in which different proteins are fluorescently labeled, and physically associate or dissociate to generate or abolish a FRET signal. Class IV sensors have been developed to investigate the dynamics of small molecules such as the second messenger 3',5'-cyclic adenosine monophosphate (cAMP, ref. 23). GFP has also been used in the intermolecular FRET mode with other non-GFP fluorophores, such as in measurement of PKC α (24) and Rac 1 (25) activities.

2.3. NEW GREEN AND RELATED FLUORESCENT PROTEINS

2.3.1. GFP Mutants

The available repertoire of genetically-encoded autofluorescent proteins for sensor design has expanded rapidly. Early random and rational mutagenesis of GFP yielded spectrally distinct GFP variants, referred to as blue, cyan and yellow fluorescent proteins (BFP, CFP and YFP, reviewed in ref. 3). Recent GFP mutagenesis efforts have been directed at generating mutants with longer and different wavelengths, pH-insensitivity, improved brightness and photostability, and accelerated cellular maturation. For example, a GFP variant was generated with an emission wavelength between CFP and GFP called CGFP (cyan-green fluorescent protein, ref. 26). CGFP is essentially pH-insensitive in the physiological range, making it suitable for targeting to acidic organelles and an excellent partner in FRET-based sensors. New YFPs have been reported with

improved characteristics for cellular applications (27-29). The YFP mutant Citrine (YFP-V68L/Q69M, ref. 27) is chloride-insensitive, more photostable, and less pH-sensitive than the original YFP. The YFP mutant Venus (P46L/F64L/M153T/V163A/S175G, ref. 28) has the favorable characteristics of Citrine as well as improved brightness and folding efficiency.

2.3.2. Novel Fluorescent Proteins

Naturally-occurring fluorescent proteins from non-bioluminescent Anthozoa species have been cloned which have high homology to GFP (30). Of the six native proteins cloned by Matz *et al.*, two had fluorescence emission maxima at longer wavelengths (up to 583 nm) than available GFP mutants; a red fluorescent protein (drFP583, λ_{em} 583 nm) was commercialized by Clontech as DsRed. Although extending the spectral range of genetically-encoded fluorescent proteins, DsRed undergoes tetramerization (31, 32) and its red fluorescence in cells develops slowly (up to 30 hours) as the green fluorescence from immature DsRed disappears (31). A DsRed mutant with ~10-fold more rapid maturation has been generated (33), as well as mutants with less propensity to aggregate (34, 35). Strategies to reduce DsRed aggregation have also been reported that involve the co-expression of the untagged or GFP-tagged protein of interest in addition to the DsRed-tagged protein, however, these methods may not be generally applicable to all systems (36-38).

In addition to the fluorescent proteins described by Matz *et al.*, (30) several fluorescent and non-fluorescent colored proteins have been cloned from other Anthozoa (39-41). A fluorescent protein from *Entacmaea quadricolor* (eqFP11) has several favorable properties, including red-shifted fluorescence emission (611 nm) with a large Stokes' shift (52 nm), low green fluorescence of its immature form, relatively rapid maturation (~12 hours), and pH-insensitivity (41); however, like DsRed, eqFP11 undergoes oligomerization. A non-fluorescent purple protein was cloned from the sea anemone *Anemonia sulcata*, which when mutated yielded a fluorescent protein with an emission wavelength of 595 nm (42). This strategy of mutating non-fluorescent proteins has been applied to other non-fluorescent GFP homologs to produce fluorescent proteins with emission wavelengths as long as 645 nm (43), one of which is available commercially from Clontech as HcRed. Many new fluorescent proteins are becoming available for cell biological applications and development of new sensors (for review, see refs. 44, 45). The discovery and characterization of these proteins has also motivated novel applications such as fluorescent 'stopwatches' and photoactivatable proteins that emit at different wavelengths upon activation (46-48). A more complete biochemical and biophysical characterization of these proteins is probably required before they are ready for incorporation into fluorescent protein-based sensors.

2.4. GFP-BASED SENSORS

2.4.1. pH Sensors

The chromophore of many green fluorescent proteins is intrinsically pH sensitive. The GFP chromophore consists of three amino acids that are post-translationally modified by cyclization and oxidation (3, 49). The wildtype GFP chromophore, *p*-

hydroxybenzylideneimidazolinone, is created by modification of the genetically-encoded residues serine-tyrosine-glycine at positions 65–67. The resulting phenolic group within the chromophore can be titrated but is not directly accessible to solvent (50). Many GFP mutants are pH-sensitive, with different pK_a 's depending on chromophore composition and the nature of surrounding amino acids. The intrinsic pH sensitivity of GFPs has been exploited to measure cytoplasmic and organellar pH non-invasively. Four GFP mutants containing the S65T mutation (which favors formation of the phenolate chromophore that absorbs at longer wavelengths than the neutral form) were characterized with pK_a values of 4.8–6.1 (1). A pH titration for purified recombinant GFP-S65T is shown in Figure 2.2A. Biophysical characterization of these proteins indicated that the pH response was rapid (<ms), reversible, and involved a ground-state effect. Calibration experiments in whole cells using ionophores indicated that the fluorescent proteins faithfully report pH *in vivo* (Figure 2.2B) and non-invasive measurements of cytoplasmic, mitochondrial and Golgi pH were carried out. Additional GFP mutants were also characterized and used to measure cellular pH changes. One of the GFP mutants used by Llopis *et al.* (2) for measurement of mitochondrial pH was YFP, which had an apparent pK_a value of 7.1; however, subsequent studies showed that YFP is also halide-sensitive and thus not suitable for cellular pH measurements (5, 6). A direct comparison of GFP with the established pH-sensitive dye BCECF provided direct validation for the use of GFP as a cytoplasmic pH indicator (51).

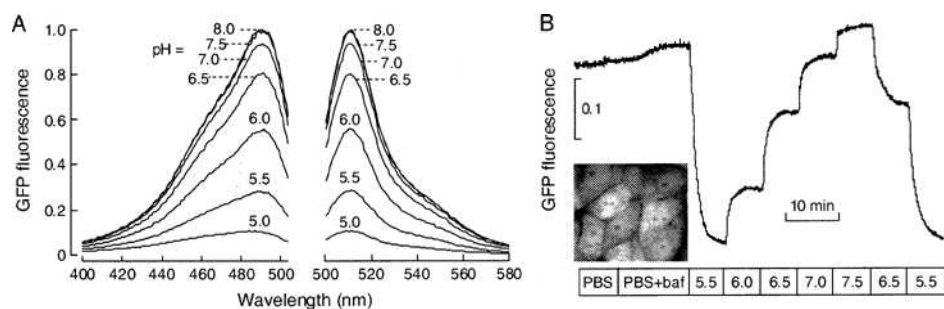


Figure 2.2. Sensitivity of intrinsic GFP fluorescence to pH. **A.** Fluorescence excitation and emission spectra of purified recombinant GFP-S65T as a function of solution pH. **B.** Demonstration that GFP-S65T fluorescence is pH sensitive in cells. GFP-S65T was expressed in cell cytoplasm and nucleoplasm of fibroblasts. Cell fluorescence was monitored continuously from a group of cells (inset) during perfusion with saline ('PBS') and saline containing ionophores ('PBS + baf') to equalize cytoplasmic and solution pH at indicated values. Adapted from ref. 1.

Ratioable probes are desirable for fluorescence microscopy since fluorescence ratios do not depend on expression levels, cell depth, illumination intensity, and non-uniform probe distribution. Miesenböck *et al.*, (52) reported ratioable pH sensors (called pHluorins) that were identified by random mutagenesis of residues that interact with the GFP chromophore. Fluorescence of the pHluorins is pH-sensitive with a reciprocal fluorescence response for the excitation wavelengths 395 and 475 nm in the pH range 5.5–7.5. Targeting of pHluorins to synaptic vesicles in neurons permitted the dynamic

study of individual fusion events and synaptic vesicle cycling during neurotransmitter secretion at nerve terminals (52, 53). A family of ratioable, single excitation/dual-emission GFP pH sensors (called deGFPs) have also been described with pK_a values of 6.8–8.0 (54, 55). These sensors have cysteine residue substitutions at position 148 and/or 203 as well as threonine substitution at position 65. The fluorescence emission from deGFPs increases at ~460 nm and decreases at ~515 nm as pH decreases (54). Also, ratiometric pH sensors based on the fusion of two differentially pH-sensitive GFPs have been reported (56). These sensors (called GFpH and YFpH) had pK_a values of 6.1 and 6.8, respectively, and could be used either in single excitation or dual excitation FRET modes. These probes were used to measure cytoplasmic pH and local changes in pH at endosomal surfaces (when fused to the α_{1B} -adrenergic receptor) during norepinephrine-stimulated endocytosis.

2.4.2. Chloride/Halide Sensors

It was recognized that the fluorescence of YFP, but not other forms of GFP, was intrinsically sensitive to halides including chloride (5). The halide-sensing mechanism of one mutant, YFP-H148Q, was investigated and applications to living cells were developed (6). Halide binding produces an increase in the pK_a of YFP-H148Q (from ~7 to 8 for 0–400 mM chloride), such that its fluorescence at constant pH decreases with increasing halide concentration. When expressed in cell cytoplasm, YFP-H148Q fluorescence provided a useful read-out of cytoplasmic halide concentration suitable for measurement of halide transport processes. However, a limitation of YFP-H148Q was its relative weak chloride sensitivity, with 50% decrease in fluorescence at 100 mM Cl⁻ at pH 7.5. A subsequent structural study identified the putative YFP halide binding site (57).

To overcome this limitation, YFPs with greatly improved halide sensitivity (for Cl⁻ and I⁻), random mutagenesis was carried out of residue pairs in the vicinity of the halide binding site (58). A YFP mutant (H148Q/I152L) was identified with very high iodide sensitivity ($K_1 \sim 3$ mM at pH 7.5, Figure 2.3A) and rapid fluorescence response to changes in halide concentration (figure inset). Like YFP-H148Q, the halide-sensing mechanism of mutants involved pK_a shifts (Figure 2.3B). Figure 2.3C shows large, reversible changes in cell fluorescence in response to Cl⁻/I⁻ exchange.

A useful application of YFPs has been in drug discovery for the identification of compounds that activate or inhibit the cystic fibrosis transmembrane conductance regulator (CFTR) chloride/halide channel. Figure 2.4A shows the strategy for identification of CFTR activators by high-throughput screening (59). Cells co-expressing human CFTR and a YFP indicator are subjected to an iodide gradient in a fluorescence plate reader. Pre-addition of an activator results in increased iodide entry and YFP fluorescence quenching. Figure 2.4B shows representative data from a 96-well plate. Fluorescence changed little in the saline (no activator) control. Addition of a known CFTR activator (apigenin) resulted in decreased fluorescence, as did some (~50 out of 60,000) of the test compounds (Figure 2.4B). More than a dozen novel CFTR activators were identified with novel chemical structures and sub-micromolar activating potencies, two of which are shown in Figure 2.4C. A similar screening strategy was applied recently to identify potent CFTR inhibitors, which function as antidiarrheals to prevent cholera toxin-induced intestinal fluid secretion (60).

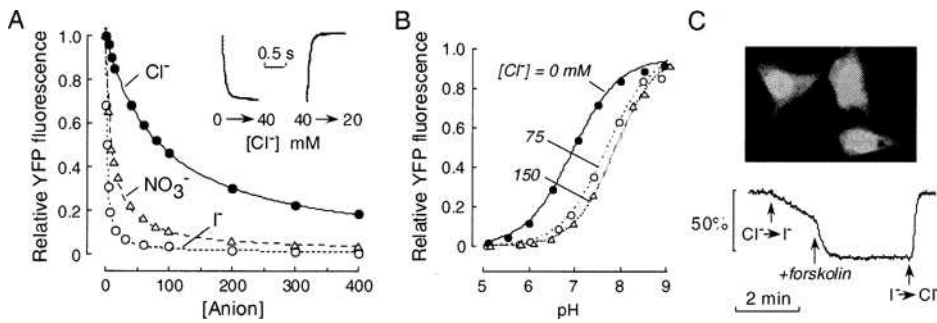


Figure 2.3. YFPs with improved halide sensitivity. A. Titration of purified YFP-H148Q/I152L with indicated anions at pH 7.4. Inset: Stopped-flow fluorescence kinetics showing rapid response to changes in [Cl⁻]. B. pH titration of YFP-H148Q/I152L at indicated [Cl⁻] showing pK_a shift. C. (top) Fluorescence micrograph of CFTR-expressing cells showing cytoplasmic YFP indicator. (bottom) Time course of cell fluorescence showing reversible decrease in fluorescence in response to I⁻ influx. Forskolin elevates cAMP and activates CFTR halide transport. Adapted from ref. 58.

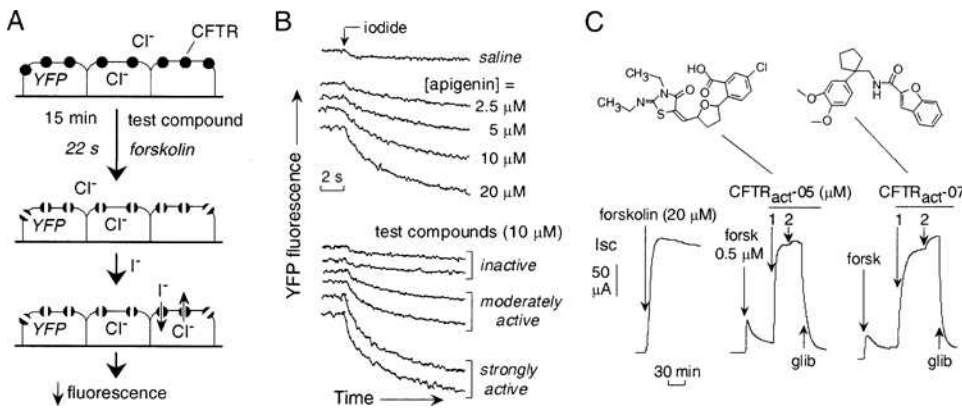


Figure 2.4. Identification of CFTR activators by high-throughput screening using YFP indicator. A. Screening strategy. FRT cells expressing YFP-H148Q and human CFTR were subjected to an inward I⁻ gradient after adding test compound (out of 60,000 small molecules) and a low concentration of forskolin. Activated CFTR permits I⁻ influx resulting in decreased fluorescence. B. Representative data from single wells of 96-well plates showing cell fluorescence in response to I⁻ addition without activators ('saline'), with a known activator ('apigenin') and with various test compounds having different levels of activity. C. Short-circuit current electrophysiology showing induction of strong CFTR currents by sub-micromolar concentrations of two CFTR activators discovered by the screening. Adapted from ref. 59.

A FRET-based ratiometric halide sensor has been generated by the fusion of CFP and YFP (61). The YFP moiety was chloride-sensitive as described above. The emission ratio of this sensor changed from ~2.0 at 0 mM chloride to ~0.5 at 500 mM chloride with

50% change at 160 mM chloride. This probe was used in neurons to measure temporal changes in chloride concentration during development and in response to GABA stimulation.

2.4.3. Sensors of Protease Activity

FRET-based GFP sensors for protease activity have been generated by genetically inserting protease consensus sequences between GFP donor/acceptor partners; protease-mediated cleavage of the consensus sequence irreversibly abolishes FRET. In a first report in 1996 a probe for Factor X_a protease activity was generated using this paradigm and validated for measurement of protease activity *in vitro* (14). Such sensors have been proven to provide robust readouts of protease activity using cell sorting (62), plate reader (63) and image (64) detection methods. Although FRET efficiency is generally deduced from steady-state donor/acceptor fluorescence intensities, cross-correlation analysis (15) and lifetime imaging (to obviate the requirement for fluorescent proteins to be spectrally resolvable, ref. 65) have also been applied to measure protease activity. Recently, sensors using CFP and the Venus variant of YFP (28) have been used to investigate the progression of caspase activity during apoptosis (16). Although a similar study had been reported (66), the newly designed probes did not suffer from pH- and halide- dependent changes in fluorescence. Caspase-3 activity in the cytosol was shown to precede activity in the nucleus, with maximal nuclear activity of caspase-3 at ~10 minutes. The kinetics of caspase-9 activation were slower and predominated in the cytosol; however, the progression of morphological changes after activation of both caspases were similar, suggesting concurrent activation during apoptosis.

2.4.4. Calcium Sensors

The use of fluorescent proteins to design FRET-based intramolecular sensors was stimulated by Tsien and colleagues with their design of the 'cameleon' sensors to investigate the dynamics of the second messenger calcium (17). The initial cameleons - so called because the sensor 'readily changes color and retracts and extends a long tongue (M13) into and out of the mouth of the calmodulin' - consisted of two spectrally distinct fluorescent proteins joined by a specialized calcium-sensing linker composed of calmodulin (CaM), a CaM-binding peptide (M13) and a short, flexible linker. Calcium binding to the CaM moiety and subsequent CaM binding to M13 results in a reorientation of the two fluorescent proteins, typically cyan and yellow, altering FRET efficiency. The calcium binding affinity of these sensors can be altered by mutagenesis of the CaM moiety. Cameleon-2 was used to detect calcium transients in HeLa cells in response to histamine and the purinergic agonist ATP, with ~25 % change in emission ratio (maximal cytoplasmic [Ca²⁺] of ~3 μ M), nearly half the full dynamic range of this sensor (~60 %). Lower affinity cameleons targeted to the endoplasmic reticulum (ER) reported resting calcium concentrations ([Ca²⁺] ~ 60–400 μ M) and calcium mobilization in response to histamine stimulation with similar changes in emission ratios.

To overcome the pH-sensitivity of the YFP moiety second generation cameleons were developed in which the mutations V68L and Q69K were introduced into YFP to reduce its pK_a from ~7 to 6 (18). More recently, cameleons were rationally re-engineered with a new linker region based on structural information from NMR studies of CaM

bound to CaM-dependent kinase fragment (67). This new sensor had a two-fold increase in the FRET dynamic range for $[Ca^{2+}]$ in the range 50–1000 nM.

The general applicability of cameleons to detect changes in $[Ca^{2+}]$ has been demonstrated in diverse organisms. Calcium-mediated exocytosis was investigated by genetic fusion of cameleons to phogrin, a protein localized to the secretory granule membranes, which permitted the measurement of cytoplasmic $[Ca^{2+}]$ at the vesicle surface in pancreatic β cells (68). It was reported that vesicles near the plasma membrane (within $\sim 1 \mu\text{m}$) experienced greater apparent changes in $[Ca^{2+}]$ than vesicles far from the cell surface. Targeting of cameleons to the nucleus, ER and mitochondria have permitted investigation of calcium transients in these organelles in response to cell signaling, cell death and circadian rhythms (69–73). Allen *et al.* (74) investigated calcium signaling in *Arabidopsis* using cameleons, demonstrating stimulus-specific calcium oscillations accompanying stomatal closure. Two-photon fluorescence excitation has been used with cameleons in cell cultures (75), and in a study of calcium transients during muscle contraction in transgenic nematode worms expressing cameleons in the pharyngeal muscle (76). Further developments of cameleons will likely include the use of different FRET partners, such as red fluorescent proteins (77, 78), and use of environmentally-insensitive YFPs such as Citrine and Venus (27–29).

Calcium sensors using modified single GFPs (class II sensors) have also been reported. These sensors were developed using circularly permuted fluorescent proteins or information derived from circular permutation studies about the intrinsic structural malleability of fluorescent proteins (for example see ref. 7). An indicator containing a CaM domain at position Y145 of YFP, termed 'camgaroo 1' because it carries a smaller companion (CaM) inserted in its pouch, has an apparent K_d for calcium of 7 μM and a Hill coefficient of 1.6. Spectroscopic studies indicated that deprotonation of the chromophore with increasing $[Ca^{2+}]$ was responsible for the calcium-dependent changes in fluorescence intensity. In cell cultures camgaroo-1 reported changes in $[Ca^{2+}]$ in response to various maneuvers including histamine; however, despite a large dynamic range the response of camgaroo 1 to physiological stimuli was modest ($\sim 5\%$, ref. 7). The general applicability of this insertional paradigm was further demonstrated by the insertion of a zinc finger motif into the same YFP location, giving a zinc sensor (7). First and second generation camgaroos (27) have been used to measure calcium transients in *Drosophila* mushroom bodies in response to depolarization and cholinergic stimulation (79) and to investigate the role of voltage-dependent anion channels in mitochondrial Ca^{2+} homeostasis (80).

Additional class II calcium sensors have been reported by two groups. Nakai *et al.* (8) generated a sensor (termed G-CaMP) using a circularly permuted GFP (with a new amino-terminus at residue 148) containing CaM at its carboxy-terminus and M13 at its amino-terminus. G-CaMP has a low K_d for calcium of 235 nM (~ 30 times lower than of camgaroo), large changes in fluorescence intensity in response to physiological changes in $[Ca^{2+}]$ (~ 5 -fold change for 0–1 mM calcium) and rapid response kinetics. In an elegant study, G-CaMP was used with two-photon fluorescence microscopy to map odor perception in *Drosophila* brain (81). Miyawaki and colleagues (9) reported a similar calcium sensor called pericam (permuted YFP and a CaM) based upon YFP. Here, circularly permuted YFP (new amino-terminus at residue 144 with V68L/Q69K mutations to confer pH-insensitivity) contained amino-terminus M13 and carboxy-terminus CaM domains. Refinement of the pericam sensors by mutagenesis gave 'flash-pericam' and 'inverse-pericam' which become more and less bright, respectively, upon

calcium binding, as well as a 'ratiometric-pericam' (mutations Y203F and H148D) suitable for dual excitation, single emission ratio imaging. These probes have apparent K_d for calcium of 0.2–1.7 μM and Hill coefficients of ~ 1 . Calcium transients in the cytosol, nucleus and mitochondria were visualized with ratiometric-pericam in response to physiologically relevant stimuli (9). Pericams have also been used to investigate the relationship between cytosolic and mitochondrial calcium in beating ventricular myocytes from neonatal rats (82), and to measure calcium changes in pancreatic islet β cells in response to glucose and kinase activity (83).

2.4.5. Sensors of Calcium-Calmodulin

The group of Persechini developed a FRET-based sensors of free $(\text{Ca}^{2+})_4$ -CaM concentration exploiting essentially the same components of calcium signaling as used in the cameleons: CaM and a CaM binding fragment (17 amino acids from smooth muscle myosin light chain kinase CaM binding domain, ref. 84). $(\text{Ca}^{2+})_4$ -CaM binding to the CaM binding fragment linking donor/acceptor GFPs results in reduced FRET efficiency. Indicator protein and CaM were microinjected in an initial study which demonstrated that the activity of a typical CaM target (affinity ~ 1 nM) was responsive to physiological changes calcium concentration (84). The relationship between free calcium and $(\text{Ca}^{2+})_4$ -CaM was investigated using stably transfected cell lines expressing similar indicator moieties (85). No $(\text{Ca}^{2+})_4$ -CaM was detected below 0.2 mM free calcium and the maximum concentration of $(\text{Ca}^{2+})_4$ -CaM was determined to be ~ 45 nM (85). Local intracellular differences in free $(\text{Ca}^{2+})_4$ -CaM concentrations were found and it was speculated that these differences may provide a mechanism for selective activation of CaM dependent signaling process (86).

2.4.6. Sensors of Other Second Messengers

The main target of cAMP is the holotetrameric enzyme protein kinase A (PKA), which mediates process such as transcription, metabolism and secretion/absorption via protein phosphorylation. Binding to cAMP the regulatory subunit of PKA causes dissociation from the catalytic subunit, providing a strategy for engineering of a GFP-based cAMP FRET sensor (23). Two fusion proteins were generated, the first between the PKA catalytic subunit and GFP, and the second between the PKA regulatory subunit and BFP; cAMP binding results in subunit dissociation and reduced FRET efficiency. A similar strategy was described originally for a microinjectable cAMP sensor in which PKA subunits were chemically labeled with small organic molecules (87). The GFP-based cAMP sensor could detect increases in cAMP in cell culture models in response to cAMP agonists, giving ~ 30 % increase in the donor-to-acceptor emission ratio. Improved cAMP sensors were subsequently developed using CFP and YFP to study cAMP compartmentalization and organization in PKA-mediated signaling (88). Discrete regions of increased cAMP were found in cardiac myocytes (at transverse tubule/junctional sarcoplasmic reticulum) in response to β -adrenergic stimulation, resulting from restricted cAMP diffusion, PKA anchoring, and phosphodiesterase activity.

GFP-based sensors have been developed for the second messenger 3',5'-cyclic guanosine monophosphate (cGMP) (89, 90). Nitric oxide and various hormones and

toxins stimulate guanylyl cyclases to convert guanosine triphosphate (GTP) to cGMP, which activates cGMP-dependent kinases, cyclic nucleotide-gated channels and phosphodiesterases. The first reported cGMP sensor consisted of the cGMP-binding domain from cGMP-dependent protein kinase Ia (with residues 1–47 removed) interposed between cyan and yellow fluorescent proteins (89). A similar probe was reported in which the first 77 amino acids of cGMP-dependent protein kinase Ia were removed (90). Exposure of cells expressing the sensor of Sato *et al.* (89) to 1 mM 8-Br-cGMP (a cell permeable and phosphodiesterase resistant cGMP analog) or nitric oxide (NO) release produced a 20–30 % decrease in the cyan-to-yellow emission ratio, indicating increased FRET efficiency. The probe of Honda *et al.* (90) gave a similar signal size in response to NO release, but in the opposite direction.

A GFP-based sensor for nitric oxide (NO), termed FRET-MT, was generated by inserting metallothionein (MT) between CFP and YFP (91). MT is a cysteine-rich metal binding protein implicated in intracellular redox and NO signaling. NO decreased the emission ratio (yellow-to-cyan) of FRET-MT due to conformational changes in MT upon formation of nitrosothiol groups with cysteines and displacement of MT-bound metal ions. In support of this mechanism, metal ion chelation from MT resulted in a similar reduction in FRET-MT emission ratio. Application of the NO donor S-nitrosylglutathione in endothelial cells reduced FRET-MT emission ratio. This system was used to investigate changes in NO after muscarinic agonists (carbachol and bradykinin) and calcium ionophores.

A class II sensor for the second messenger inositol 1,4,5-triphosphate (IP_3) has been reported (92). IP_3 mediates intracellular calcium mobilization and is generated by hormone and neurotransmitter stimulated phospholipase C metabolism of phosphatidylinositol-4,5-bisphosphate (PIP_2). In contrast to other GFP-based sensors, the fluorescence 'readout' of this probe is a spatial distribution profile within the cell. The IP_3 sensor is composed of GFP fused to the pleckstrin homology (PH) domain (termed GFP-PHD). PH domains bind both membrane-associated PIP_2 and cytoplasmic IP_3 but the affinity for IP_3 is ~20-fold higher. As such, generation of IP_3 is reported by translocation of GFP-PHD from the plasma membrane to the cytoplasm. Microinjection of IP_3 increased cytoplasmic GFP-PHD, whereas overexpression of IP_3 5-phosphatase abolished agonist-induced cytoplasmic translocation of GFP-PHD, verifying that GFP-PHD was reporting increased IP_3 and not PIP_2 disappearance. This sensor was used to correlate IP_3 dynamics and cytoplasmic calcium (using fura-2), identifying calcium and IP_3 waves in single cells and between cells.

2.4.7. Sensors of Protein Kinase Activity

Several groups have described class III GFP-based sensors to investigate the kinetics and spatial organization of protein kinase activity during signal transduction. The general strategy has been to insert a phosphorylation consensus sequence between GFP donor/acceptor pairs such that conformation changes upon protein phosphorylation alter FRET efficiency. A PKA activity sensor was engineered by fusing blue and green fluorescent proteins with the PKA target domain from the cAMP response element binding protein (21). PKA-mediated phosphorylation yielded ~25 % changes in fluorescence emission ratio. The kinetics, spatial organization and effect of inhibitors on PKA-mediated signaling were investigated. Improved kinase sensors were designed by incorporating phosphoamino-binding domains into the linker region along with the kinase

substrate consensus sequences (22, 93, 94). Upon phosphorylation of the kinase consensus sequence, the phosphoamino-binding domain induced conformational changes in the linker domain. For example, a PKA sensor was engineered using CFP and citrine joined by the 14–3–3 τ phosphoserine/threonine binding domain and a 21 amino acid kinase substrate domain (22). The maximum change in emission ratio for this probe was ~30 % for physiological stimuli *in vivo*. Sensors for the specific tyrosine kinase activities of Src, Abl, epidermal growth factor (EGF) receptor, and insulin signaling have been generated using linkers composed of Src homology (SH) 2 domains (to bind phosphotyrosine) and specific kinase consensus substrates (93, 94).

An alternative strategy to generate a sensor of tyrosine kinase activity has been described involving insertion of the complete CrkII protein between CFP and YFP (95). CrkII functions as an 'adaptor protein' in signal transduction cascades initiated by EGF, nerve growth factor (NGF) and insulin-like growth factor-I. The CrkII adaptor contains phosphotyrosine-binding SH2 and enzyme-binding SH3 domains. In response to tyrosine kinase activation, CrkII delivers specific SH3-bound enzymes to activated phosphotyrosine-containing proteins at the plasma membrane via SH2-mediated interactions. CrkII is also phosphorylated at tyrosine 221 during signal transduction. An intramolecular interaction between a SH2 domain and phosphotyrosine-221 produces a conformational change in CrkII, giving an ~60 % change in emission ratio. Although not specific for a single kinase, this sensor could be used to investigate the subset of CrkII mediated signal transduction processes and was applied to investigate the spatial and temporal organization of EGF stimulation *in vivo*.

Fluorescence lifetime imaging (FLIM) has been used to study the spatial and temporal activation of protein kinases using GFP-tagged kinases. To investigate the activation of protein kinase Ca (PKC α) a two component assay system was developed consisting of GFP-tagged PKC α and a (microinjected) Cy3-labeled antibody specific for a phosphothreonine present in activated PKC α (24). Activation of PKC α and threonine phosphorylation resulted in antibody-PKC α interaction and reduction in GFP lifetime by GFP-Cy3 energy transfer. Treatment of fibroblasts with phorbol esters was shown to activate PKC α in punctate regions near the plasma membrane. Using this same FLIM technique Bastiaens and colleagues (96) investigated activation of the dimeric receptor tyrosine kinase ErbB1. Cells expressing GFP-tagged ErbB1 were microinjected with a Cy3-antibody specific for a phosphotyrosine present in the activated ErbB1 receptor. After cell stimulation with bead-immobilized EGF, rapid widespread ErbB1 activation was observed as reported by decreased GFP lifetime. It was suggested that ErbB1 dimers were transient and that ligand-independent propagation of receptor activation was an important additional amplification step in ErbB1 signaling.

2.4.8. Sensors of G proteins

G proteins, such as those of the Ras family, are involved in many signal transduction pathways. G proteins cycle between active GTP bound and inactive GDP bound forms, with exchange controlled by activating guanine nucleotide exchange factor (GEF) and deactivating GTPase activating protein (GAP). GFP-based sensors have been engineered to investigate the spatial organization of G protein activation. Class III-type probes were designed in which CFP and YFP were linked using a Ras moiety (Ras or Rap 1) and the Ras-binding domain of Raf (Raf RBD). Ras activation by GEF increases FRET efficiency as Ras and Raf RBD interact, whereas Ras inactivation by GAP eliminates the

Ras-Raf RBD interaction and reduces FRET efficiency (97). The activation patterns of Ras and Rap 1 were found to differ in EGF-stimulated fibroblasts and NGF-stimulated PC12 cells: Rap 1 was activated intracellularly in perinuclear region, whereas Ras was activated at the cell periphery.

An alternative FRET strategy was developed to investigate another Ras-type GTPase called Rac 1 (25). A GFP-Rac 1 fusion was used in conjunction with fluorescently-tagged p21-binding domain (PBD, derived from p21-activated kinase 1) that binds selectively to the GTP-bound form of Rac 1. Cells expressing the GFP-Rac1 fusion were microinjected with the fluorescently tagged-PBD; Rac 1 activation and PBD-Rac 1 interaction resulted in GFP FRET to the acceptor dye (Alexa 546). This strategy was used to show that platelet derived growth factor stimulation of Rac 1 in fibroblasts was greatest in membrane ruffles (25). Rac 1 activity was also found to be important in mechano-sensitive signal transduction and chemotaxis (98, 99).

GFP-based sensors have also been engineered to investigate the activity of Ran, a member of the Ras family of GTPases with possible roles in mitosis and nuclear transport of importins (100). It was predicted that Ran-GTP is found only in interphase nuclei or close to mitotic chromosomes because of discrete localization of Ran-GEF and Ran-GAP. Two FRET-based sensors were developed to investigate Ran activities. The first sensor (YRC), designed to monitor the nucleotide-binding status of Ran, was composed of YFP and CFP joined by the Ran-binding domain (RBD) from the yeast Ran-GAP accessory factor Yrb1; RBD selectively binds Ran-GTP which reduces the FRET efficiency. The second sensor contained an importin binding domain in the linker such that importin sequestration by Ran-GTP produced increase FRET. These sensors were used to investigate Ran-GTP gradients in mitotic *Xenopus* extracts.

2.4.9. Metabolite Sensors

FRET-based intramolecular GFP sensors have been developed recently to measure metabolite concentrations and to investigate the subcellular distribution of metabolites (19, 20). Components of the gram-negative bacterial metabolite sensing apparatus, the periplasmic binding proteins (PBPs), were used to link CFP and YFP to generate sensors called FLIPs (fluorescent indicator proteins). FLIPs selective for maltose (FLIPmals) were engineered using mutated maltose binding protein inserts to yield sensors that are able to measure maltose concentrations from 0.3 to 2000 μM (19). The FLIPmal sensors were used to measure maltose concentrations in beer and uptake of maltose by yeast cells (19). A similar strategy was applied to measure glucose in fibroblasts using a sensor containing a glucose/galactose binding insert (20). Cytoplasmic glucose concentration was found to vary over ~ 2 orders of magnitude in response to changes in external glucose in the physiological range (0.5–10 mM), and was decreased in response 2-deoxyglucose and cytochalasin B.

2.4.10. Sensors of Reduction-Oxidation (Redox) Potential

A sensor of redox potential was generated by Østergaard *et al.* (101) by addition of redox-sensitive cysteines at positions 149 and 202 of YFP. Under oxidative conditions the fluorescence of this redox sensor was reduced by approximately 50 % as a consequence of decreased absorption by the chromophore. High-resolution crystallographic studies of the sensor indicated that formation of a disulfide bond

between the reactive cysteine residues resulted in rearrangement of amino acids in the vicinity of the chromophore and deformation of the β -barrel structure, presumably causing the observed changes in fluorescence. The redox potential of the engineered cysteine residues, -261 mV, is within the physiological range for other redox-active cysteines. When expressed in *E. coli*, this sensor reported the oxidative state of the cytoplasm and distinguished between wildtype and an isogenic strain lacking thioredoxin reductase which resulted in a more oxidative cytoplasm.

2.4.11. Nitration Sensors

GFP has been used as an intrinsic sensor of protein nitration, a post-translational modification observed in several neurological diseases including Parkinson's Disease, as well as in inflammation (102-104). Nitration decreases GFP fluorescence as a result of the formation of a 3-nitrotyrosyl adduct in the chromophore (105); this process is irreversible, sensitive ($IC_{50} \sim 20 \mu M$) and dependent upon the concentration of nitration agent (as opposed to cumulative exposure effects). This property of GFP was used *in vivo* to investigate proposed mechanisms of protein nitration. It was concluded that oxidation and nitration are not necessarily coupled *in vivo*.

2.4.12. Voltage Sensors

GFP-based sensors that report changes in membrane potential have been developed. The first sensor described was constructed by ligating GFP in the Shaker potassium channel between the last membrane-spanning domain and the carboxy-terminal region (Figure 2.5A, ref. 10). The Shaker channel was mutated to prevent ion conductance whilst maintaining voltage-sensitive structural changes. When expressed in oocytes, the fractional change in fluorescence evoked by changes in membrane potential for this sensor was small (Figure 2.5B). It was proposed that structural rearrangements in Shaker were responsible for changes in fluorescence, as fluorescence changes correlated with channel gating. Different GFP variants were subsequently incorporated at the same position in Shaker and mutation of Shaker was performed to generate new sensors with altered spectra, kinetics and voltage dependence (106). For instance, the ecliptic GFP variant had much faster response kinetics (10 ms vs. 100 ms, Figure 2.5C) and the L336A mutant of Shaker responded better at negative potentials than the original sensor.

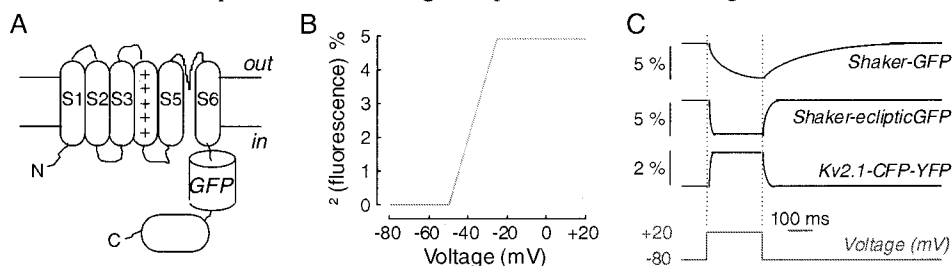


Figure 2.5. GFP-based sensors of cell membrane potential. **A.** Schematic of a Shaker-based membrane potential sensor. GFP was inserted after the last membrane-spanning region and before the carboxy-terminal region of Shaker. **B.** Relationship between percentage fluorescence change and membrane potential for Shaker-

based voltage sensor. C. Fluorescence responses to an applied depolarization pulse for Shaker-based sensors (*top two curves*) and FRET-based sensors containing a portion of Kv1.2. Adapted from refs. 10, 106 and 107.

A FRET based membrane potential sensor was generated by the tandem fusion of CFP and YFP to the carboxy-terminus of the Kv2.1 potassium channel (107). Membrane potential changes were proposed to result in structural rearrangements of the channel protein altering CFP/YFP relative orientation. This sensor has sub-millisecond response kinetics for depolarization (-80 to 20 mV), however, the magnitude response of this sensor to voltage changes was quite low (~2 % / 100 mV, Figure 2.5C, ref. 107). Recently a GFP-based membrane potential sensor was engineered using the voltage-gated rat μ I skeletal sodium channel having rapid response but small voltage-dependent changes in fluorescence (11).

2.5. PERSPECTIVE AND FUTURE DIRECTIONS

Application of GFP and related genetically-encoded fluorescent proteins to the engineering of fluorescent sensors has significantly advanced our understanding of many cell biological process. As discussed, GFP-based sensors are non-invasive, stable and can be genetically targeted to specific cell types or organelles. These features offer distinct advantages over existing small molecule indicators. Recent advances have improved the specificity of GFP-sensors after appreciating the sensitivity of the fluorescence of some GFPs to pH, chloride and other factors.

To date, GFP-based sensors have been extensively applied to investigate signal transduction. Sensors of kinase activity, second messengers and G proteins have been used to investigate many aspects of cell signaling. In addition, sensors have been developed to measure enzyme activities, membrane potential, redox-state, protease activity, and metabolite concentrations. However, GFP-based sensors for other molecules of intermediary metabolism, such as ATP, phosphocreatine, and phosphate, which are not yet available, would be extremely useful in understanding metabolic organization in cells. Although ATP can be detected using luminescence assays (108-110), many of these molecules are at present only visible to nuclear magnetic resonance (NMR) which has poor sensitivity and spatial resolution. GFP-sensors have also been described for the metal ions calcium and zinc, as well as halides, but not for the many other small ions and molecules in cells.

Finally, technological advances should further exploit the unique advantages of GFP-sensors. Transgenic expression of GFP-based sensors in whole animals can provide a wealth of information about cell function *in vivo*. Two-photon fluorescence excitation has improved optical penetration depths for non-invasive *in vivo* measurements. New long-wavelength fluorescent proteins should further expand the possible sensor application in whole animals and plants.

2.6. ACKNOWLEDGMENTS

Supported by grants EB00415, HL73856, HL59198, DK35124 and EY13574 from the National Institutes of Health, and Research Development Program grant R613 and a CF Drug Discovery grant from the Cystic Fibrosis Foundation.

2.7. REFERENCES

1. M. Kneen, J. Farinas, Y. Li, and A.S. Verkman, Green fluorescent protein as a noninvasive intracellular pH indicator, *Biophys. J.* **74**, 1591-1599 (1997).
2. J. Llopis, J.M. McCaffery, A. Miyawaki, M.G. Farquhar, and R.Y. Tsien, Measurement of cytosolic, mitochondrial, and Golgi pH in single living cells with green fluorescent proteins, *Proc. Natl. Acad. Sci. USA* **95**, 6803-6808 (1998).
3. R.Y. Tsien, The green fluorescent protein, *Annu. Rev. Biochem.* **67**, 509-544 (1998).
4. M.-A. Elsliger, R.M. Wachter, G.T. Hanson, K. Kallio, and S.J. Remington, Structural and spectral response of green fluorescent protein variants to changes in pH, *Biochemistry* **38**, 5296-5301 (1999).
5. R.M. Wachter and S.J. Remington, Sensitivity of the yellow variant of green fluorescent protein to halides and nitrate, *Curr. Biol.* **9**, R628-R629 (1999).
6. S. Jayaraman, P. Haggie, R.M. Wachter, S.J. Remington, and A.S. Verkman, Mechanism and cellular application of a green fluorescent protein-based halide sensor, *J. Biol. Chem.* **275**, 6047-6050 (2000).
7. G.S. Baird, D.A. Zacharias, and R.Y. Tsien, Circular permutation and receptor insertions within green fluorescent proteins, *Proc. Natl. Acad. Sci. USA* **96**, 11241-11246 (1999).
8. J. Nakai, M. Ohkura, and K. Imoto, A high signal-to-noise Ca^{2+} probe composed of a single green fluorescent protein, *Nat. Biotech.* **19**, 137-141 (2001).
9. T. Nagai, A. Sawano, E.S. Park, and A. Miyawaki, Circularly permuted green fluorescent proteins engineered to sense Ca^{2+} , *Proc. Natl. Acad. Sci. USA* **98**, 3197-3202 (2001).
10. M.S. Siegel and E.Y. Isacoff, A genetically encoded optical probe of membrane voltage, *Neuron* **19**, 735-741 (1997).
11. K. Ataka and V.A. Pieribone, A genetically targetable fluorescent probe of channel gating with rapid kinetics, *Biophys. J.* **82**, 509-516 (2002).
12. U. Heinemann and M. Hahn, Circular permutation of polypeptide chains: implications for protein folding and stability, *Prog. Biophys. Mol. Biol.* **64**, 121-143 (1995).
13. S. Topell, J. Henncke, and R. Glockshuber, Circularly permuted variants of the green fluorescent protein, *FEBS Lett.* **457**, 283-289 (1999).
14. R.D. Mitra, C.M. Silva, and D.C. Youvan, Fluorescence resonance energy transfer between blue-emitting and red-shifted excitation derivatives of the green fluorescent protein, *Gene* **173**, 13-17 (1996).
15. T. Kohl, K.G. Heinze, R. Kuhlemann, A. Koltermann, and P. Schuille, A protease assay for two-photon crosscorrelation and FRET analysis based on fluorescent proteins, *Proc. Natl. Acad. Sci. USA* **99**, 12161-12166 (2002).
16. K. Takemoto, T. Nagai, A. Miyawaki, and M. Miura, Spatio-temporal activation of caspase revealed by indicator that is insensitive to environmental effects, *J. Cell Biol.* **160**, 235-243 (2003).
17. A. Miyawaki, J. Llopis, R. Heim, J.M. McCaffery, J.A. Adams, M. Ikura, and R.Y. Tsien, Fluorescent indicators for Ca^{2+} based on green fluorescent proteins and calmodulin, *Nature* **388**, 882-887 (1997).
18. A. Miyawaki, O. Giesbeck, R. Heim, and R.Y. Tsien, Dynamic and quantitative Ca^{2+} measurements using improved cameleons, *Proc. Natl. Acad. Sci. USA* **96**, 2135-2140 (1999).
19. M. Fehr, W.B. Frommer, and S. Lalonde, Visualization of maltose uptake in living yeast cells by fluorescent nanosensors, *Proc. Natl. Acad. Sci. USA* **99**, 9846-9851 (2002).
20. M. Fehr, S. Lalonde, L. I., M.W. Wolff, and W.B. Frommer, In vivo imaging of the dynamics of glucose uptake in the cytosol of COS-7 cells by fluorescent nanosensors, *J. Biol. Chem. In Press* (2003).
21. Y. Nagai, M. Miyazaki, R. Aoki, T. Zama, S. Inouye, K. Hirose, M. Iino, and M. Hagiwara, A fluorescent indicator for visualizing cAMP-induced phosphorylation in vivo, *Nat. Biotech.* **18**, 313-316 (2000).
22. J. Zhang, Y. Ma, S.S. Taylor, and R.Y. Tsien, Genetically encoded reporters of protein kinase A activity reveal impact of substrate tethering, *Proc. Natl. Acad. Sci. USA* **98**, 14997-15002 (2001).
23. M. Zaccolo, F.D. Georgi, C.Y. Cho, T.K. L. Feng, P.A. Negulescu, S.S. Taylor, R.Y. Tsien, and T. Pozzan, A genetically encoded, fluorescent indicator for cyclic AMP in living cells, *Nat. Cell Biol.* **2**, 25-29 (2000).
24. T. Ng, A. Squire, G. Hansra, F. Bornancin, C. Prevostel, A. Hanby, W. Harris, D. Barnes, S. Schmidt, H. Mellor, P.I. Bastiaens, and P.J. Parker, Imaging protein kinase Ca activation in cells, *Science* **283**, 2085-2089 (1999).
25. V.S. Kraynov, C. Chamberlain, G.M. Bekoch, M.A. Schwartz, S. Slabaugh, and K.M. Hahn, Localized Rac activation in living cells, *Science* **290**, 333-337 (2000).
26. A. Sawano and A. Miyawaki, Directed evolution of green fluorescent proteins by a new versatile PCR strategy for site-directed and semi-random mutagenesis, *Nuc. Acids Res.* **28**, E78 (2000).

27. O. Greisbeck, G.S. Baird, R.E. Campbell, D.A. Zacharias, and R.Y. Tsien, Reducing the environmental sensitivity of yellow fluorescent protein, *J. Biol. Chem.* **276**, 29188-29194 (2001).
28. T. Nagai, K. Ibata, E.S. Park, M. Kubota, K. Mikoshiba, and A. Miyawaki, A variant of yellow fluorescent protein with fast and efficient maturation for cell-biological applications, *Nat. Biotech.* **20**, 87-90 (2002).
29. A. Rekas, J.-R. Alattia, T. Nagai, A. Miyawaki, and M. Ikura, Crystal structure of Venus, a yellow fluorescent protein with improved maturation and reduced environmental sensitivity, *J. Biol. Chem.* **277**, 50573-50578 (2002).
30. M.V. Matz, A.F. Fradkov, Y.A. Labas, A.P. Savitsky, A.G. Zarskiy, M.L. Markelov, and S.A. Lukyanov, Fluorescent proteins from nonbioluminescent Anthozoa species, *Nat. Biotech.* **17**, 969-973 (1999).
31. G.S. Baird, D.A. Zacharias, and R.Y. Tsien, Biochemistry, mutagenesis, and oligomerization of DsRed, a red fluorescent protein from coral, *Proc. Natl. Acad. Sci. USA* **97**, 11984-11989 (2000).
32. D. Yarbough, R.M. Wachter, K. Kallio, M.V. Matz, and S.J. Remington, Refined crystal structure of DsRed, a red fluorescent protein from coral, at 2.0-Å resolution, *Proc. Natl. Acad. Sci. USA* **98**, 462-467 (2001).
33. B.J. Bevis and B.S. Glick, Rapidly maturing variants of the Discosoma red fluorescent protein (DsRed), *Nat. Biotech.* **20**, 83-87 (2002).
34. R.E. Campbell, O. Tour, A.E. Palmer, P.A. Steinbach, G.S. Baird, D.A. Zacharias, and R.Y. Tsien, A monomeric red fluorescent protein, *Proc. Natl. Acad. Sci. USA* **99**, 7877-82 (2002).
35. Y.G. Yanushevich, D.B. Staroverov, A.P. Savitsky, A.F. Fradkov, N.G. Gurskaya, M.E. Bulina, K.A. Lukyanov, and S.A. Lukyanov, A strategy for the generation of non-aggregating mutants of Anthozoa fluorescent proteins, *FEBS Lett.* **511**, 11-14 (2002).
36. P. Gavin, R.J. Devenish, and M. Prescott, An approach for reducing unwanted oligomerization of DsRed fusion proteins, *Biochem. Biophys. Res. Comm.* **298**, 707-713 (2002).
37. U. Lauf, P. Lopez, and M.M. Falk, Expression of fluorescently tagged connexins: a novel approach to rescue function of oligomeric DsRed-tagged proteins, *FEBS Lett.* **498**, 1-5 (2001).
38. A. Soling, A. Simm, and N. Rainov, Intracellular localization of Herpes simple virus type 1 thymidine kinase fused to different fluorescent proteins depends on choice of fluorescent tag, *FEBS Lett.* **527**, 153-158 (2002).
39. Y.A. Labas, N.G. Gurskaya, Y.G. Yanushevich, A.F. Fradkov, K.A. Lukyanov, S.A. Lukyanov, and M.V. Matz, Diversity and evolution of the green fluorescent protein family, *Proc. Natl. Acad. Sci. USA* **99**, 4256-4261 (2002).
40. J. Wiedenmann, C. Elke, K.-D. Spindler, and W. Funke, Cracks in the b-can: Fluorescent proteins from *Anemonia sulcata* (Anthozoa, Actinaria), *Proc. Natl. Acad. Sci. USA* **97**, 14091-14096 (2000).
41. J. Wiedenmann, A. Schenk, C. Röcker, A. Girod, K.-D. Spindler, and G.U. Nienhaus, A far-red fluorescent protein with fast maturation and reduced oligomerization tendency from *Entacmea quadricolor* (Anthozoa, Actinaria), *Proc. Natl. Acad. Sci. USA* **99**, 11646-11651 (2002).
42. K.A. Lukyanov, A.F. Fradkov, N.G. Gurskaya, M.V. Matz, Y.A. Labas, A.P. Savitsky, M.L. Markelov, A.G. Zarskiy, X. Zhao, Y. Fang, W. Tan, and S.A. Lukyanov, Natural animal coloration can be determined by a nonfluorescent green fluorescent protein homolog, *J. Biol. Chem.* **275**, 25879-25882 (2000).
43. G. Gurskaya, A. Fradkov, A. Tersikh, M.V. Matz, Y.A. Labas, V.I. Martynov, Y.G. Yanushevich, K.A. Lukyanov, and S.A. Lukyanov, GFP-like chromoproteins as a source of far-red fluorescent proteins, *FEBS Lett.* **507**, 16-20 (2001).
44. M.V. Matz, K.A. Lukyanov, and S.A. Lukyanov, Family of green fluorescent protein: journey to the end of the rainbow, *BioEssays* **24**, 953-959 (2002).
45. A. Miyawaki, Green fluorescent protein-like proteins in reef Anthozoa animals, *Cell Struct. Func.* **27**, 343-347 (2002).
46. A. Tersikh, A.F. Fradkov, G. Ermakova, A.G. Zarskiy, P. Tan, A.V. Kajava, X. Zhao, S.A. Lukyanov, M.V. Matz, S. Kim, I. Weissman, and P. Siebert, "Fluorescent timer": Protein that changes color with time, *Science* **290**, 1585-1588 (2000).
47. V.V. Verkhusha, H. Otsuna, T. Awasaki, H. Oda, S. Tsukita, and K. Ito, An enhanced mutant of red fluorescent protein DsRed for double labeling and developmental timer of neural fiber bundle formation, *J. Biol. Chem.* **276**, 29621-29624 (2001).
48. D.M. Chudakov, V.V. Belousov, A.G. Zarskiy, V.V. Novoselov, D.B. Staroverov, D.B. Zorov, S.A. Lukyanov, and K.A. Lukyanov, Kindling fluorescent proteins for precise in vivo photolabeling, *Nat. Biotech.* **21**, 191-194 (2003).
49. B.G. Reid and G.C. Flynn, Chromophore formation in green fluorescent protein, *Biochemistry* **36**, 6786-6791 (1997).
50. M. Örmö, A.B. Cubitt, K. Kallio, L.A. Gross, R.Y. Tsien, and S.J. Remington, Crystal structure of the *Aequorea victoria* green fluorescent protein, *Science* **273**, 1392-1395 (1996).

51. R.B. Robey, O. Ruiz, A.V.P. Santo, J. Ma, F. Kear, L.-J. Wang, C.-J. Li, A.A. Bernado, and J.A.L. Arruda, pH-Dependent fluorescence of a heterologously expressed Aequorea green fluorescent protein mutant: in situ spectral characteristics and applicability to intracellular pH estimation, *Biochemistry* **37**, 9894-9901 (1998).
52. G. Miesenböck, D.A. De Angelis, and J.E. Rothman, Visualizing secretion and synaptic transmission with pH-sensitive green fluorescent proteins, *Nature* **394**, 192-195 (1998).
53. S. Sankaranarayanan, D.A. De Angelis, G. Rothman, and T.A. Ryan, The use of pHluorins for optical measurements of presynaptic activity, *Biophys. J.* **79**, 2199-2208 (2000).
54. G.T. Hanson, T.B. McAnaney, E.S. Park, M.E.P. Rendall, D.K. Yarbough, S. Chu, L. Xi, S.G. Boxer, M.H. Montrose, and S.J. Remington, Green fluorescent protein variants as ratiometric dual emission pH sensors. 1. Structural characterization and preliminary application, *Biochemistry* **41**, 15477-15488 (2002).
55. T.B. McAnaney, E.S. Park, G.T. Hanson, S.J. Remington, and S.G. Boxer, Green fluorescent protein variants as ratiometric dual emission pH sensors. 2. Excited-state dynamics, *Biochemistry* **41**, 15489-15494 (2002).
56. T. Awaji, A. Hirasawa, H. Shirakawa, G. Tsujimoto, and S. Miyazaki, Novel green fluorescent protein-based ratiometric indicators for monitoring pH in defined intracellular microdomains, *Bioch. Biophys. Res. Comm.* **289**, 457-462 (2001).
57. R.M. Wachter, D. Yarbough, K. Kallio, and S.J. Remington, Crystallographic and energetic analysis of binding of selected anions to the yellow variants of green fluorescent protein, *J. Mol. Biol.* **301**, 157-171 (2001).
58. L.J. Galletta, P.M. Haggie, and A.S. Verkman, Green fluorescent protein-based halide indicators with improved chloride and iodide affinities, *FEBS Letts.* **499**, 220-224 (2001).
59. T. Ma, L. Vetrivel, H. Yang, N. Pedemonte, O. Zegarra-Moran, L.J. Galletta, and A.S. Verkman, High-affinity activator of cystic fibrosis transmembrane conductance regulator (CFTR) chloride conductance identified by high-throughput screening, *J. Biol. Chem.* **277**, 37235-37241 (2002).
60. T. Ma, J.R. Thiagarajah, H. Yang, N.D. Sonawane, C. Folli, L.J. Galletta, and A.S. Verkman, Thiazolidinone CFTR inhibitor identified by high-throughput screening blocks cholera toxin-induced intestinal fluid secretion, *J. Clin. Invest.* **110**, 1651-1658 (2002).
61. T. Kuner and G. Augustine, A genetically encoded ratiometric indicator for chloride: capturing chloride transients in cultured hippocampal neurons, *Neuron* **27**, 447-459 (2000).
62. X. Xu, A.L.V. Gerard, B.C.B. Huang, D.C. Anderson, D.G. Payan, and Y. Luo, Detection of programmed cell death using fluorescence energy transfer, *Nuc. Acids Res.* **26**, 2034-2035 (1998).
63. J. Jones, R. Heim, J. Stack, and B.A. Pollok, Development and application of a GFP-FRET intracellular caspase assay for drug screening, *J. Biomol. Screen.* **5**, 307-318 (2000).
64. P.W. Vanderklish, L.A. Krushel, B.H. Holst, J.A. Gally, K.L. Crossin, and G.M. Edelman, Marking synaptic activity in dendritic spines with a calpain substrate exhibiting fluorescence resonance energy transfer, *Proc. Natl. Acad. Sci. USA* **97**, 2253-2258 (1999).
65. A.G. Harpur, F.S. Wouters, and P.I. Bastiaens, Imaging FRET between spectrally similar GFP molecules in single cells, *Nat. Biotech.* **19**, 167-169 (2001).
66. N.P. Mahajan, D.C. Harrison-Shostak, J. Michaux, and B. Herman, Novel mutant green fluorescent protein protease substrates reveal the activation of specific caspases during apoptosis, *Chem. Biol.* **6**, 401-409 (1999).
67. K. Truong, A. Sawano, H. Mizuno, H. Hama, K.I. Tong, T.K. Mal, A. Miyawaki, and F. M. Ikura, FRET-bases in vivo Ca^{2+} imaging by a new calmodulin-GFP fusion molecule, *Nat. Struct. Biol.* **8**, 1069-1073 (2001).
68. E. Emmanouilidou, A.G. Teschemacher, A.E. Pouli, L.I. Ncholls, E.P. Seward, and G.A. Rutter, Imaging Ca^{2+} concentration changes at the secretory vesicle surface with a recombinant targeted cameleon, *Curr. Biol.* **9**, 915-918 (1999).
69. D.N. Bowser, S. Petrou, R.G. Panchal, M.L. Smart, and D.A. Williams, Release of mitochondrial Ca^{2+} via the permeability transition activates endoplasmic reticulum Ca^{2+} uptake, *FASEB J.* **16**, 1105-1107 (2002).
70. R. Foyouzi-Youssefi, S. Arnaudeau, C. Borner, W.L. Kelley, J. Tschopp, D.P. Lew, N. Demaurex, and K.-H. Krause, Bcl-2 decreases the free Ca^{2+} concentration within the endoplasmic reticulum, *Proc. Natl. Acad. Sci. USA* **97**, 5723-5728 (2000).
71. M. Ikeda, T. Sugiyama, C.S. Wallace, H.S. Gompf, T. Yoshioka, A. Miyawaki, and C.N. Allen, Circadian dynamic of cytosolic and nuclear Ca^{2+} in single suprachiasmatic nucleus neurons, *Neuron* **38**, 253-263 (2003).
72. M. Jaconi, C. Bony, S.M. Richards, A. Terzic, S. Arnaudeau, G. Vassort, and M. Pucéat, Inositol 1,4,5-risphosphate directs Ca^{2+} flow between mitochondria and the endoplasmic/sarcoplasmic reticulum: A role in regulating cardiac autonomic Ca^{2+} spiking, *Mol. Biol. Cell* **11**, 1845-1858 (2000).

73. R. Yu and P.M. Hinkle, Rapid turnover of calcium in the endoplasmic reticulum during signaling, *J. Biol. Chem.* **275**, 23648-23653 (2000).
74. G.J. Allen, S.P. Chu, K. Schumaker, C.T. Shimazaki, D. Vefeados, A. Kemper, S.D. Hawke, G. Tallman, R.Y. Tsien, J.F. Harper, J. Chory, and J.I. Schroeder, Alteration of stimulus-specific guard cell calcium oscillations and stomatal closing in *Arabidopsis det3* mutant, *Science* **289**, 2338-2342 (2000).
75. G.Y. Fan, H. Fujisaki, A. Miyawaki, R.-K. Tsay, R.Y. Tsien, and M.H. Ellisman, Video-rate scanning two-photon excitation fluorescence microscopy and ratio imaging with cameleons, *Biophys. J.* **76**, 2412-2420 (1999).
76. R. Kerr, V. Lev-Ram, G. Baird, P. Vincent, R.Y. Tsien, and W.R. Schafer, Optical imaging of calcium transients in neurons and pharyngeal muscle of *C. elegans*, *Neuron* **26**, 583-594 (2000).
77. A. Miyawaki, H. Mizuno, T. Nagai, and A. Sawano, Development of genetically encoded fluorescent indicators for calcium, *Meth. Enzymol.* **360**, 202-225 (2003).
78. H. Mizuno, A. Sawano, P. Eli, H. Hama, and A. Miyawaki, Red fluorescent protein from *Discosoma* as a fusion tag and partner for fluorescence energy transfer, *Biochemistry* **40**, 2502-2510 (2001).
79. D. Yu, G. Baird, R.Y. Tsien, and R.L. Davis, Detection of Calcium transients in *Drosophila* mushroom body neurons with Camgario reporters, *J. Neuro.* **23**, 64-72 (2003).
80. E. Rapizzi, P. Pinton, G. Szabadkai, M.R. Wieckowski, G. Vandecasteele, G. Baird, R.A. Tuft, K.E. Fogarty, and R. Rizzuto, Recombinant expression of the voltage-dependent anion channel enhances the transfer of Ca^{2+} microdomains to mitochondria, *J. Cell Biol.* **159**, 613-624 (2002).
81. J.W. Wang, A.M. Wong, J. Flores, L.B. Vosshall, and R. Axel, Two-photon calcium imaging reveals an odor-evoked map of activity in the fly brain, *Cell* **112**, 271-282 (2003).
82. V. Robert, P. Gurlini, V. Tosello, T. Nagai, A. Miyawaki, F. Di Lisa, and T. Pozzan, Beat-to-beat oscillations of mitochondrial $[\text{Ca}^{2+}]$ in cardiac cells, *EMBO J.* **20**, 4998-5007 (2001).
83. P. Pinton, T. Tsuboi, E.K. Ainscow, T. Pozzan, R. Rizzuto, and G.A. Rutter, Dynamics of glucose-induced membrane recruitment of protein kinase c bII in living pancreatic islet b-cells, *J. Biol. Chem.* **277**, 37702-37710 (2002).
84. V.A. Romoser, P.M. Hinkle, and A. Persechini, Detection in living cells of Ca^{2+} -dependent changes in the fluorescence emission of an indicator composed of two green fluorescent protein variants linked by a calmodulin-binding sequence. A new class of fluorescent indicators, *J. Biol. Chem.* **272**, 13270-13274 (1997).
85. A. Persechini and B. Cronk, The relationship between the free concentration of Ca^{2+} and Ca^{2+} -calmodulin in intact cells, *J. Biol. Chem.* **27**, 6827-6830 (1999).
86. M.N. Teruel, W. Chen, A. Persechini, and T. Meyer, Differential codes for free Ca^{2+} -calmodulin signals in the nucleus and cytosol, *Curr. Biol.* **10**, 86-94 (2000).
87. S.R. Adams, A.T. Harootunian, Y.J. Beuchler, S.S. Taylor, and R.Y. Tsien, Fluorescence ratio imaging of cAMP in single cells, *Nature* **349**, 694-697 (1991).
88. M. Zaccolo and T. Pozzan, Discrete Microdomains with high concentration of cAMP in stimulated rat neonatal cardiac myocytes, *Science* **295**, 1711-1715 (2002).
89. M. Sato, N. Hida, T. Ozawa, and Y. Umezawa, Fluorescent indicators for cyclic GMP based on cyclic GMP-dependent protein kinase Ia and green fluorescent protein, *Anal. Chem.* **72**, 5918-5924 (2000).
90. A. Honda, S.R. Adams, C.L. Sawyer, V. Lev-Ram, R.Y. Tsien, and W.R.G. Dostman, Spatiotemporal dynamics of guanosine 3',5'-cyclic monophosphate revealed by a genetically encoded fluorescent indicator, *Proc. Natl. Acad. Sci. USA* **98**, 12437-12442 (2001).
91. L.L. Pearce, R.E. Gandle, W. Han, K. Wasserlso, M. Stitt, A.J. Kanai, M.K. McLaughlin, B.R. Pitt, and E.S. Levitan, Role of metallothionein in nitric oxide signaling as revealed by green fluorescent fusion protein, *Proc. Natl. Acad. Sci. USA* **97**, 477-482 (2000).
92. K. Hirose, S. Kadowaki, M. Tanabe, H. Takeshima, and M. Iino, Spatiotemporal dynamics of inositol 1,4,5-triphosphate that underlies complex Ca^{2+} mobilization patterns, *Science* **284**, 1527-1530 (1999).
93. M. Sato, T. Ozawa, K. Inukai, T. Asano, and Y. Umezawa, Fluorescent indicators for imaging protein phosphorylation in single living cells, *Nat. Biotech.* **20**, 287-294 (2002).
94. A.Y. Ting, K.H. Kain, R.L. Klemke, and R.Y. Tsien, Genetically encoded fluorescent reporters of protein tyrosine kinase activities in living cells, *Proc. Natl. Acad. Sci. USA* **98**, 15003-15008 (2001).
95. K. Kurokawa, N. Mochizuki, Y. Ohba, H. Mizuno, A. Miyawaki, and M. Matsuda, A pair of fluorescent energy transfer-based probes for tyrosine phosphorylation of the CrkII adaptor protein *in vivo*, *J. Biol. Chem.* **276**, 31305-31310 (2001).
96. P.J. Verveer, F.S. Wouters, A.R. Reynolds, and P.I. Bastiaens, Quantitative imaging of lateral ErbB1 receptor signal propagation in the plasma membrane, *Science* **290**, 1567-1570 (2000).
97. M. Mochizuki, S. Yamashita, K. Kurokawa, Y. Ohba, T. Nagai, A. Miyawaki, and M. Matsuda, Spatio-temporal images of growth-factor-induced activation of Ras and Rap1, *Nature* **411**, 1065-1068 (2001).

98. A. Katsumi, J. Milanini, W.B. Kiosses, M.A. del Pozo, R. Kaunas, S. Chien, K.M. Hahn, and M.A. Schwartz, Effect of cell tension on the small GTPase Rac, *J. Cell Biol.* **158**, 153-164 (2002).
99. E.M. Gardiner, K.N. Pestonjamas, B.P. Bohl, C. Chamberlain, K.M. Hahn, and G.M. Bokoch, Spatial and temporal analysis of Rac activation during live neutrophil chemotaxis, *Curr. Biol.* **12**, 2029-2034 (2002).
100. P. Kalab, K. Weis, and R. Heald, Visualization of a Ran-GTP gradient in interphase and mitotic Xenopus egg extracts, *Science* **295**, 2452-2456 (2002).
101. H. Østergaard, A. Henriksen, F.G. Hansen, and J.R. Winther, Shedding light on disulfide bond formation: engineering a redox switch in green fluorescent protein, *EMBO J.* **20**, 5853-5862 (2001).
102. J. Beckman, A.G. Estevez, J.P. Crow, and L. Barbeito, Superoxide dismutase and death of motoneurons in ALS, *Trends Neurosci.* **24**, S15-S20 (2001).
103. B.I. Giasson, J.E. Duda, I.V. Murray, Q. Chen, J.M. Souza, H.I. Hurt, H. Ischiropoulos, J.Q. Trojanowski, and V.M. Lee, Oxidative damage linked to neurodegeneration by selective α -synuclein nitration in synucleinopathy lesions, *Science* **290**, 985-989 (2000).
104. H. Ischiropoulos and J.S. Beckman, Oxidative stress and nitration in neurodegeneration: Cause, effect, or association?, *J. Clin. Invest.* **111**, 163-169 (2003).
105. M.G. Espey, S. Xavier, D.D. Thomas, K.M. Miranda, and D.A. Wink, Direct real-time evaluation of nitration with green fluorescent protein in solution and within human cells reveals the impact of nitrogen dioxide vs. peroxynitrite mechanisms, *Proc. Natl. Acad. Sci. USA* **99**, 3481-3486 (2002).
106. G. Guerrero, M.S. Siegel, B. Roska, E. Loots, and E.Y. Isacoff, Tuning FlaSh: redesign of the dynamics, voltage range and color of the genetically encoded optical sensor of membrane potential, *Biophys. J.* **83**, 3607-3618 (2002).
107. R. Sakai, V. Repunte-Canonigo, C.D. Raj, and T. Knöpfel, Design and characterization of a DNA-encoded, voltage sensitive fluorescent protein, *Eur. J. Neurosci* **13**, 2314-2318 (2001).
108. H.J. Kennedy, A.E. Pouli, E.K. Ainscow, L.S. Jouaville, R. Rizzuto, and G.A. Rutter, Glucose generates sub-plasma membrane ATP microdomains in single islet b-cells. Potential role for strategically located mitochondria, *J. Biol. Chem.* **274**, 13281-13291 (1999).
109. P. Magalhães and R. Rizzuto, Mitochondria and calcium homeostasis: a tale of three luminescent proteins, *Luminescence* **16**, 67-71 (2001).
110. A.M. Porcelli, P. Pinton, E.K. Ainscow, A. Chiesa, M. Rugolo, G.A. Rutter, and R. Rizzuto, Targeting of reporter molecules to mitochondria to measure calcium, ATP, and pH, *Methods Cell Biol.* **65**, 353-380 (2001).

Advanced Concepts in Fluorescence Sensing

Part B: Macromolecular Sensing

Geddes, C.D.; Lakowicz, J.R. (Eds.)

2005, XIII, 300 p. 146 illus., 3 illus. in color., Hardcover

ISBN: 978-0-387-23644-5